PHILOSOPHICAL TRANSACTIONS OF THE ROYAL SOCIETY A MATHEMATICAL, PHYSICAL & ENGINEERING SCIENCES

Texture and Stress Determination in Metals by Using Ultrasonic Rayleigh Waves and Neutron Diffraction [and Discussion]

C. M. Sayers, D. R. Allen, G. E. Haines, G. G. Proudfoot, H. N. G. Wadley, R. B. Thompson and E. Almond

Phil. Trans. R. Soc. Lond. A 1986 **320**, 187-200
doi: 10.1098/rsta.1986.0110

Phil. Trans. R. Soc. Lond. A **320**, 187–200 (1986)
Printed in Great Britain

Texture and stress determination in metals by using ultrasonic Rayleigh waves and neutron diffraction

By C. M. Sayers†, D. R. Allen, G. E. Haines and G. G. Proudfoot
Atomic Energy Research Establishment, Materials Physics and Metallurgy Division, Harwell OX11 0RA, U.K.

Polycrystalline metals often contain significant levels of texture and internal stress. Plastic anisotropy originates from the texture or crystallographic alignment and can affect the formability of the metal, whereas the presence of internal stress can seriously limit the lifetime of a component. In the presence of either texture or stress, the ultrasonic velocity in the material depends on the propagation and polarization directions, and there is considerable interest in exploiting this anisotropy for non-destructive texture and stress determination. In this paper an analytical expression for the angular dependence of the Rayleigh-wave velocity in polycrystalline metals with small anisotropy typical of rolled plate is given. It is shown that surface-wave velocity measurements can be combined with the normal shear-wave birefringence technique to give a texture-independent determination of the difference in principal stresses in the plane of the plate. The theory is tested by comparing ultrasonic measurements on two aluminium plates with the behaviour predicted by using a neutron diffraction determination of the crystallite orientation distribution function. The possibility of obtaining the depth profile from the frequency dependence of the Rayleigh-wave velocity is considered.

1. Introduction

In this paper it is shown that the texture and stress of polycrystalline metals may be characterized by using the velocity of ultrasonic Rayleigh waves in combination with bulk-wave velocity measurements. There is a requirement for the non-destructive measurement of texture and stress for process control and there is considerable interest in the use of ultrasonics for this purpose. For example, in a strongly textured metal the yield stress varies with direction and this can lead to non-uniform flow in deep drawing (Hatherley & Hutchinson 1979; Hutchinson 1984).

A convenient measure of the drawability of a sheet is the plastic strain ratio or r-value. This is defined as the ratio of the strains in the width and thickness directions measured on a tensile stress specimen, strained to an elongation of about 15%. The r-value depends on the angle of the specimen axis with respect to the rolling direction, and an average value r_m is defined by

$$r_m = \tfrac{1}{4}(r_0 + 2r_{45} + r_{90}), \tag{1}$$

where r_α is the r-value for a specimen cut at an angle α to the rolling direction. High values of r_m correlate with good drawability. This occurs in cubic metals if a high proportion of (111) planes lie in the plane of the sheet. A convenient measure of the plastic anisotropy in the plane of the sheet is the quantity Δr defined by

$$\Delta r = \tfrac{1}{2}(r_0 + r_{90} - 2r_{45}). \tag{2}$$

† Present address: General Research and Mathematics, Koninklijke/Shell Exploratie en Produktie Laboratorium, Volmerlaan 6, 2288 GD Rijswijk ZH, The Netherlands.

This is found to correlate with the amount of earing that occurs in deep drawing. Ears tend to form along directions perpendicular to directions of high r-value. A positive value of Δr implies earing at 0° and 90° whereas a negative value corresponds to earing at 45° to the rolling direction. The possibility of using the angular variation of the ultrasonic velocity to characterize the plastic anisotropy is suggested by the results of Stickels & Mould (1970), who showed that the angular variation of Young's modulus in the rolling plane of low carbon steel sheet correlates with that of the plastic strain ratio. It was found that the angular variation of the elastic modulus could be used to characterize the formability of the sheet. Davies *et al.* (1972), by using the crystallite orientation distribution of Roe (1965), found that both the elastic and plastic properties of an orthorhombic aggregate of cubic crystallites are determined primarily by the fourth order coefficients of this function, and therefore demonstrated that the empirical correlation of Stickels & Mould could be justified on the basis of established theories of elastic and plastic behaviour.

In addition to texture, metals often contain internal stresses, which must be added to the external stress when determining the response of a component to an applied load. In the presence of stress the ultrasonic velocity in the material depends on the propagation and polarization directions, and this may be used to evaluate the stress present. This is the basis of the shear-wave birefringence technique (Hsu 1974) which involves the measurement of the relative velocities of two orthogonally polarized shear waves propagating in the same direction. This technique is suitable for determining stresses in metals which are isotropic in the absence of stress. In the presence of texture, however, the velocity is dependent on the orientation of the propagation and polarization directions with respect to the principal texture axes, even in the absence of stress. It is shown that surface-Rayleigh-wave velocity measurements can be combined with the normal shear-wave birefringence technique to give a texture-independent determination of the difference in principal stresses in the plane of the plate. The theory is tested by comparison with measurements on two aluminium plates and the texture obtained is compared with a neutron diffraction determination of the crystallite orientation distribution function. An additional advantage in using surface Rayleigh waves is that they average over a depth of the order of the wavelength. A frequency dependent measurement will therefore allow the depth profile of the stress distribution to be determined.

2. Theory

Let $0x_1$, $0x_2$, $0x_3$ be an orthogonal set of reference axes fixed in the sample. For a rolled plate these axes could be chosen as the rolling, transverse and normal directions. The sample is assumed to have orthorhombic symmetry, i.e. it is assumed to possess three orthogonal mirror planes given by the planes x_1x_2, x_2x_3 and x_3x_1 in figure 1 (*a*). A rolled plate, for example, usually has this type of symmetry. The crystallites are assumed to have cubic symmetry. The crystallographic alignment, or texture, of the plate is most conveniently described by the crystallite orientation distribution function (CODF). This method of analysis has been developed extensively by Roe (Roe & Krigbaum 1964; Roe 1965, 1966) and by Bunge (1965, 1968). In this paper the notation of Roe will be used.

Let $0X_1$, $0X_2$, $0X_3$ be an orthogonal set of axes for a crystallite given by the (100), (010) and (001) crystallographic directions. The orientation of a given crystallite with respect to the sample axes $0x_1$, $0x_2$, $0x_3$ can be specified by the three Euler angles ψ, θ, ϕ shown in figure

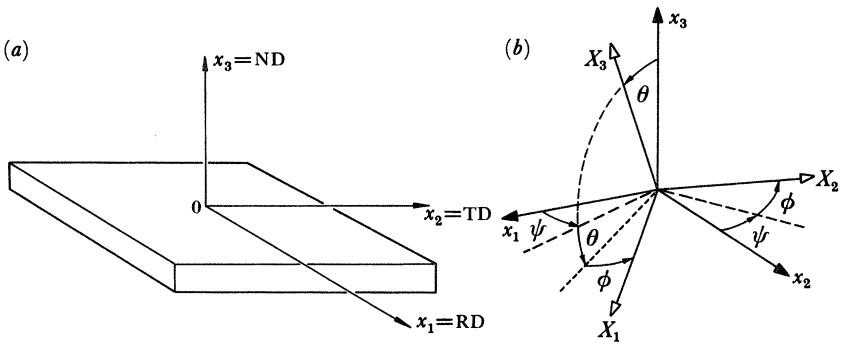

FIGURE 1 (*a*). Choice of specimen coordinate axes for a rolled plate, with $0x_1$ along the rolling direction (RD), $0x_2$ along the transverse direction (TD) and $0x_3$ along the normal direction (ND). (*b*) The orientation of the crystallite coordinate system $0X_1X_2X_3$ with respect to the sample cordinate system $0x_1x_2x_3$ given by the Euler angles ψ, θ and ϕ (Roe 1966).

1 (*b*). The CODF is denoted by $W(\xi, \psi, \phi)$ with $\xi = \cos\theta$. $W(\xi, \psi, \phi)\,\mathrm{d}\xi\,\mathrm{d}\psi\,\mathrm{d}\phi$ gives the fraction of crystallites with orientations between ξ and $\xi+\mathrm{d}\xi$, ψ and $\psi+\mathrm{d}\psi$, and ϕ and $\phi+\mathrm{d}\phi$, and is normalized such that

$$\int_0^{2\pi}\int_0^{2\pi}\int_{-1}^{1} W(\xi, \psi, \phi)\,\mathrm{d}\xi\,\mathrm{d}\psi\,\mathrm{d}\phi = 1. \tag{3}$$

It is convenient to expand $W(\xi, \psi, \phi)$ as

$$W(\xi, \psi, \phi) = \sum_{l=0}^{\infty}\sum_{m=-l}^{l}\sum_{n=-l}^{l} W_{lmn}\,Z_{lmn}(\xi)\,\exp(-im\psi)\,\exp(-in\phi), \tag{4}$$

where the Z_{lmn} are the generalized Legendre functions defined by Roe (1966). For an orthorhombic aggregate of cubic crystals the elastic constant tensor depends only on W_{400}, W_{420} and W_{440} in (4) (Pursey & Cox 1954; Bunge 1968). Explicit expressions for the elastic constants in terms of these coefficients have been given elsewhere (Morris 1969; Sayers 1982; Allen *et al.* 1983).

By using this description, the ultrasonic-wave velocities in aggregates with small anisotropy have been calculated using the variational method (Jeffreys 1961; Smith & Dahlen 1975; Aki & Richards 1980; Sayers 1985). For a linear elastic body with density ρ and elastic constants C_{ijkl}, the Lagrangian density, L, is the kinetic energy minus the elastic strain energy, and is given by

$$L = \tfrac{1}{2}\rho\dot{u}_i\,\dot{u}_i - \tfrac{1}{2}C_{ijkl}\,\epsilon_{ij}\,\epsilon_{kl}, \tag{5}$$

where a sum over repeated subscripts is understood; u_i are Cartesian components of the displacement $\boldsymbol{u} = \boldsymbol{u}(\boldsymbol{x}, t)$ of a particle from its initial position $\boldsymbol{x}$ are time t; ϵ_{ij} are components of the infinitesimal strain tensor given by

$$\epsilon_{ij} = \tfrac{1}{2}(\partial u_i/\partial x_j + \partial u_j/\partial x_i). \tag{6}$$

Hamilton's principle states that the integral of $\langle L\rangle$ is stationary for a perturbation of $\boldsymbol{u}$ about the actual motion. The angular brackets denote an average over a wavelength. The change in the ultrasonic velocity from its isotropic value may therefore be computed to first order in the anisotropy by using, as a trial field, the particle displacement in an isotropic medium. For

orthorhombic aggregates of cubic crystallites, the change $\delta v_R(\theta)$ in the Rayleigh-wave velocity from its isotropic value v_R^0 is given by

$$\delta v_R(\theta) = \tfrac{1}{2}(R_1 + R_2 \cos 2\theta + R_4 \cos 4\theta)/v_R^0 \tag{7}$$

in the absence of stress, where θ is the angle between the propagation and rolling directions (Sayers 1985). The amplitudes R_1, R_2 and R_4 are proportional to the coefficients W_{400}, W_{420} and W_{440} respectively, and are functions of Poisson's ratio, ν. Similar expressions for the change in the velocity of waves propagating in the plane of the plate, due to the presence of texture, may also be derived. Thus

$$\delta v_{SH}(\theta) \equiv v_{SH}(\theta) - v_S^0 = (\tfrac{2}{35}\sqrt{2}\pi^2 c/\rho v_S^0)\,(W_{400} - \sqrt{70}W_{440}\cos 4\theta), \tag{8}$$

$$\delta v_{SV}(\theta) \equiv v_{SV}(\theta) - v_S^0 = (\tfrac{-8}{35}\sqrt{2}\pi^2 c/\rho v_S^0)\,(W_{400} - \sqrt{\tfrac{5}{2}}W_{420}\cos 2\theta), \tag{9}$$

$$\delta v_l(\theta) \equiv v_l(\theta) - v_l^0 = (\tfrac{6}{35}\sqrt{2}\pi^2 c/\rho v_l^0)\,(W_{400} - \tfrac{2}{3}\sqrt{10}W_{420}\cos 2\theta + \tfrac{1}{3}\sqrt{70}W_{440}\cos 4\theta), \tag{10}$$

where $c = c_{11} - c_{12} - 2c_{44}$, the c_{ij} being the single crystal elastic constants. $v_{SH}(\theta)$, $v_{SV}(\theta)$ and $v_l(\theta)$ are the velocities of shear horizontal, shear vertical and longitudinal waves propagating in the plane of the plate at an angle θ to the rolling direction. v_S^0 and v_l^0 are the isotropic shear and longitudinal velocities. For propagation in the through thickness direction $0x_3$

$$\delta v_{33} \equiv v_{33} - v_l^0 = \tfrac{16}{35}(\sqrt{2}\pi^2 c/\rho v_l^0)\,W_{400}, \tag{11}$$

$$\delta v_{31} \equiv v_{31} - v_S^0 = -\tfrac{8}{35}(\sqrt{2}\pi^2 c/\rho v_S^0)\,(W_{400} - \sqrt{\tfrac{5}{2}}W_{420}), \tag{12}$$

$$\delta v_{32} \equiv v_{32} - v_S^0 = -\tfrac{8}{35}(\sqrt{2}\pi^2 c/\rho v_S^0)\,(W_{400} + \sqrt{\tfrac{5}{2}}W_{420}), \tag{13}$$

where v_{ij} is the velocity of the wave propagating in the direction $0x_i$ with polarization in the $0x_j$ direction. In the absence of stress these equations are sufficient to determine the three texture parameters W_{400}, W_{420} and W_{440}. These may then be used to plot an ultrasonic pole figure (Sayers 1982).

Let v_{Ri} denote the velocity of the Rayleigh wave propagating on the surface $x_3 = 0$ in the direction x_i. In the presence of both small texture and stress

$$\Delta v_R/v_R^0 \equiv (v_{R1} - v_{R2})/v_{R0} = (v_{R1} - v_{R2})/v_R^0|_{\text{texture}} + (v_{R1} - v_{R2})/v_R^0|_{\text{stress}}, \tag{14}$$

where, from (7)

$$(v_{R1} - v_{R2})/v_R^0|_{\text{texture}} = \tfrac{16}{7}\pi^2 c W_{420}\beta/\sqrt{5}\mu, \tag{15}$$

where β is a function of Poisson's ratio and is plotted in figure 2. λ and μ are the second-order elastic constants of the material in the isotropic limit. The stress-dependent term is given in terms of the components ϵ_{ij} of the infinitesimal strain tensor by

$$(v_{R1} - v_{R2})/v_R^0|_{\text{stress}} = (\alpha_1/2\alpha_0)\,(\epsilon_{11} - \epsilon_{22}), \tag{16}$$

α_0 and α_1 being functions of λ, μ and the third-order elastic constants ν_1, ν_2 and ν_3 (Hayes & Rivlin 1961; Hirao *et al.* 1981).

The shear-wave birefringence measurement involves the propagation of shear waves in the x_3 direction, and can be expressed, in the presence of texture and stress, by

$$\Delta v_S/v_S^0 \equiv (v_{31} - v_{32})/v_S^0 = (v_{31} - v_{32})/v_S^0|_{\text{texture}} + (v_{31} - v_{32})/v_S^0|_{\text{stress}}, \tag{17}$$

PHILOSOPHICAL TRANSACTIONS OF THE ROYAL SOCIETY A MATHEMATICAL, PHYSICAL & ENGINEERING SCIENCES

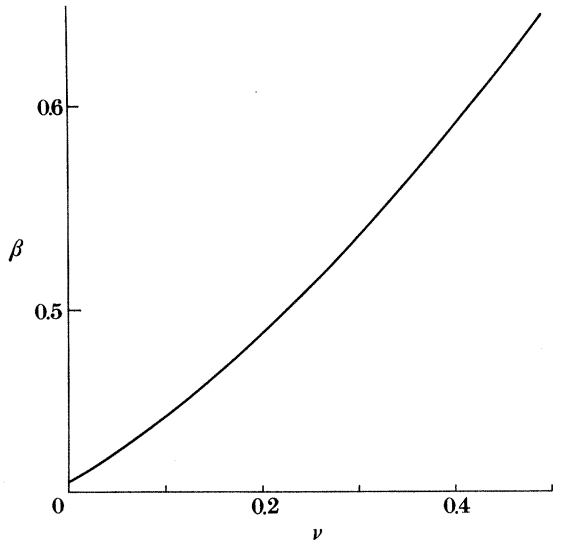

FIGURE 2. Variation of β in (15) as a function of Poisson's ratio.

where v_S^0 is the shear-wave velocity in the absence of texture and stress and v_{ij} is the velocity of a wave propagating in the direction x_i and polarized in the direction x_j. From (12) and (13)

$$(v_{31}-v_{32})/v_S^0|_{\text{texture}} = \tfrac{16}{7}\pi^2 c w_{420}/\sqrt{5}\mu, \tag{18}$$

the stress dependent term being given by

$$(v_{31}-v_{32})/v_S^0|_{\text{stress}} = (1+\nu_3/\mu)(\epsilon_{11}-\epsilon_{22}) \tag{19}$$

(Hsu 1974). Only the single texture parameter, W_{420}, appears in (14) and (17) and this may therefore be eliminated to give a texture-independent expression for the difference in principal strains $(\epsilon_{11}-\epsilon_{22})$

$$\epsilon_{11}-\epsilon_{22} = \frac{\Delta v_R/v_R^0 - \beta \Delta v_S/v_S^0}{\alpha_1/2\alpha_0 - (1+\nu_3/\mu)\beta}. \tag{20}$$

In place of the shear-wave birefringence measurement, the angular dependence of either the sv or longitudinal-wave velocity, for propagation in the plane of the plate, may be used in combination with the Rayleigh-wave velocity to eliminate the texture parameter W_{420}. This follows from (9) from which one obtains

$$(v_{13}-v_{23})/v_S^0 = \tfrac{16}{7}\pi^2 c W_{420}/\sqrt{5}\mu \tag{21}$$

and from (10) which gives

$$(v_{11}-v_{22})/v_l^0 = -\tfrac{16}{7}\pi^2 c W_{420}/\sqrt{5}(\lambda+2\mu). \tag{22}$$

3. Experiment

(a) *Samples*

Two samples were used for the ultrasonic and neutron measurements. The first was a 99.5% pure aluminium plate (BS 1470/1050A) measuring 625 mm × 530 mm × 50 mm. The second was an Al–4.5% Mg alloy plate (BS 1470/5083/0) measuring 540 mm × 530 mm × 50 mm. Both plates were cut from larger plates measuring 2000 mm × 1000 mm × 50 mm as received from the manufacturers.

(b) *Ultrasonic velocity measurements*

Three types of ultrasonic velocity measurement have been made with Rayleigh waves and SH waves travelling in the plane of the plate, and shear waves travelling in the through-plate thickness direction.

For the measurements involving Rayleigh waves, excitation was achieved by using a broad band commercial piezoelectric probe which uses the critical angle of refraction technique. The centre frequency of the transducer is nominally 2.5 MHz. Two electromagnetic acoustic transducers (EMATs) were used as receivers, designed to be sensitive to the particle displacement associated with the horizontal component of the Rayleigh wave. These were mounted in a rigid base which maintained a constant separation of 70 mm between the receivers. The three transducers, the piezoelectric transmitter and two EMAT receivers, all lay along the same axis. The signals from the EMATs were digitized and averaged (1024 times) separately using a Tetronix 7612D programmable digitizer and a PDP 11/23 computer. The phase delay associated with the propagation of the Rayleigh waves between the two EMATs was measured as a function of frequency, using a Fourier transform technique (Allen & Cooper 1983). By keeping the transducer separation constant for each measurement, the observed phase delay can be used to calculate the change in Rayleigh-wave velocity as a function of angle of propagation.

A similar arrangement to that adopted for the Rayleigh-wave measurements was used for the measurements involving SH waves travelling in the plane of the plate and is shown in figure 3. An SH wave was generated using a 1 MHz broadband conventional piezoelectric shear-wave probe coupled to the plate by an angled perspex shoe. The transducer was aligned to transmit horizontally polarized shear waves. Two EMAT SH wave receivers measured the phase delay at 0.5 MHz associated with the propagation of the surface-skimming SH wave between them, arising from a stimulus at the piezoelectric transmitter. As with the Rayleigh-wave technique, the phase delay was calculated by using the Fourier-transform technique (Allen & Cooper 1983), after the signals from the two EMAT receivers had been separately digitized and averaged. For a more detailed description of this arrangement, see Langman & Allen (1985).

For both sets of measurements, and the SH wave measurement in particular, it was important to use wide band operation and to analyse the two time channels separately. This is because, in the case of SH waves, the PZT transmitter, although aligned to produce critically refracted SH waves, that is SH waves propagating parallel and close to the horizontal surface, also produces significant power at other angles. Thus, reflections within the plate thickness are also detected which must not interfere with the surface-skimming SH waves.

Finally, measurements of the shear wave birefringence were made by using a conventional 2.25 MHz wideband piezoelectric transducer.

PHILOSOPHICAL TRANSACTIONS OF THE ROYAL SOCIETY A MATHEMATICAL, PHYSICAL & ENGINEERING SCIENCES

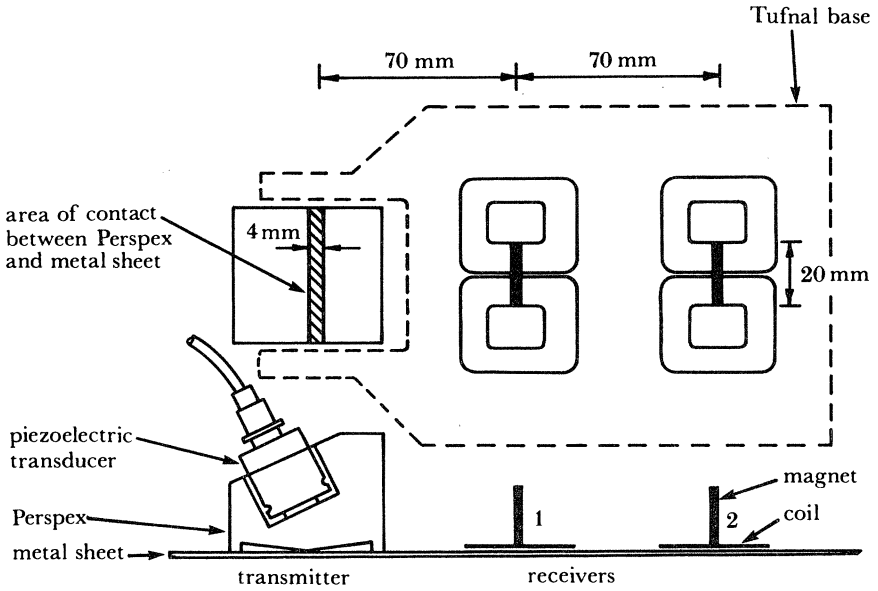

FIGURE 3. Sketch of the piezoelectric transmitter and EMAT receivers used in the SH wave measurement.

(*c*) *Neutron texture measurements*

The samples used in this investigation were 1 cm × 1 cm × 1 cm cubes cut from the plates used in the ultrasonic measurements. In a neutron-diffraction measurement of the texture, the angular distribution of the normal, $\boldsymbol{\tau}$ to a given crystallographic plane with respect to the sample axes is measured. If χ and η specify the polar and azimuthal angles of the scattering vector, $\boldsymbol{Q}$, which bisects the incident and diffracted beams, with respect to the sample coordinate system, and $I(\zeta, \eta)$ with $\zeta = \cos\chi$ is the intensity measured at orientation (ζ, η), the plane normal orientation distribution $q(\zeta, \eta)$ is defined by

$$q(\zeta, \eta) = I(\zeta, \eta) \Big/ \int_0^{2\pi} \int_{-1}^{1} I(\zeta, \eta)\, \mathrm{d}\zeta\, \mathrm{d}\eta \tag{23}$$

because $\boldsymbol{Q}$ must coincide with $\boldsymbol{\tau}$ for diffraction to occur.

The neutron diffraction measurement of the plane normal orientation distribution functions was made using the Mk VI four-circle diffractometer on the DIDO reactor at AERE Harwell. Scans of type B as described in detail by Allen *et al.* (1983) were performed. The wavelength used was 1.185 Å†. The optimum value of the scattering angle was determined experimentally for each Bragg reflection (*hkl*). The collimated counter was then fixed at this angle and the sample stepped through 684 angular positions covering the complete pole figure (Allen *et al.* 1983). The neutron count, or intensity is proportional to the volume fraction of crystallites with their (*hkl*) plane normal along the scattering vector.

† 1 Å = 10^{-1} nm = 10^{-10} m.

PHILOSOPHICAL TRANSACTIONS OF THE ROYAL SOCIETY A MATHEMATICAL, PHYSICAL & ENGINEERING SCIENCES

4. Results

(a) *Ultrasonic velocity measurements*

The angular dependence of the Rayleigh-wave velocity, given by (7), is determined by W_{420} and W_{440} of the orientation distribution function. For a stress-free plate W_{440} can be determined from the angular dependence of the velocity of SH waves travelling in the plane of the plate given by (8), this wave being a shear wave with propagation and polarization directions in the plane of the plate. Figure 4 shows a fit of this equation to the data for the aluminium and

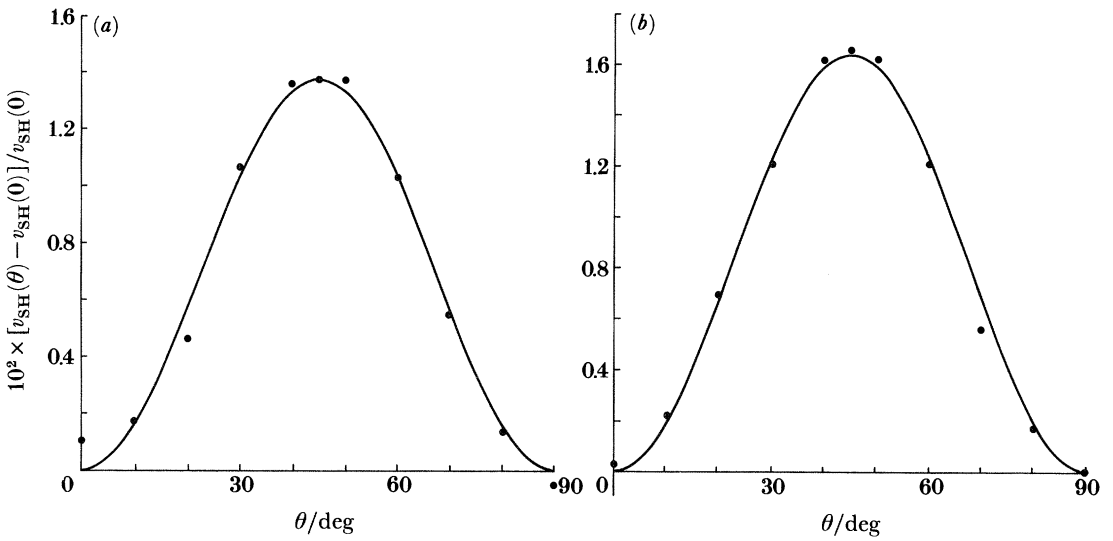

FIGURE 4. Variation of $(v_{SH}(\theta) - v_{SH}(0))/v_{SH}(0)$ with angle θ from the rolling direction for (*a*) a 99.5% pure aluminium plate and (*b*) an Al–4.5% Mg alloy.

aluminium alloy plates giving $W_{440} = -0.00256$ for the pure aluminium plate and $W_{440} = -0.00306$ for the aluminium alloy. The measured shear-wave birefringences for these two plates are $\Delta v_S/v_S^0 = 92.62 \times 10^{-4}$ and $\Delta v_S/v_S^0 = 70.32 \times 10^{-4}$, respectively, giving $W_{420} = -0.002267$ for the pure aluminium plate and $W_{420} = -0.001721$ for the alloy. Figure 5 shows the prediction of (7) using these values compared with the measured Rayleigh wave velocity made at several different frequencies. The main angular dependent term arises from the term R_2 involving W_{420}, which was obtained from the shear-wave birefringence. Because this represents a through thickness average of the texture of the plate, the low-frequency results should be in better agreement with the prediction of (7), and this is verified by the results of figure 5. With the assumption that the plates contain zero residual stress, the results suggest that both plates have a surface texture different from the bulk average. However, in contrast to the pure aluminium plate which contains a texture gradient over a thin surface layer only, the aluminium alloy plate has a texture which varies on a longer length scale. A surface residual stress different from that in the bulk would also lead to a frequency-dependent velocity similar to that seen in figure 5.

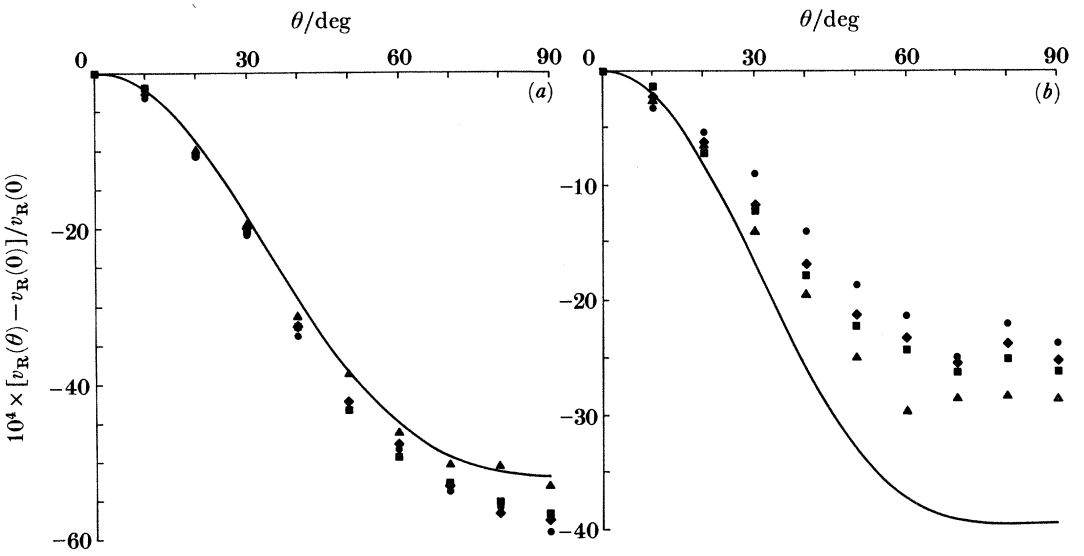

FIGURE 5. Variation of $(v_R(\theta) - v_R(0))/v_R(0)$ with angle θ from the rolling direction for (*a*) a 99.5% pure aluminium plate and (*b*) an Al–4.5% Mg alloy for several different frequencies. The curve shows the prediction of (7). ▲, 1 MHz; ■, 1.5 MHz; ◆, 2 MHz; ●, 2.5 MHz.

(*b*) *Neutron texture determination*

The (111) and (200) pole figures are most sensitive to the elastic anisotropy of the sample because these are the directions for which the single-crystal Young modulus takes its maximum and minimum values. These pole figures are shown in figure 6 for the Al–4.5% Mg alloy, and in figure 7 for the 99.5% pure aluminium plate. In these figures the rolling direction is at the top and the transverse direction at the side, the pole figure being a stereographic projection onto the rolling plane. The data is plotted directly as contours from the measured counts, minus background using a standard computer code. In contrast to the Al–4.5% Mg alloy, which shows relatively smooth contours, the pole figures for the 99.5% pure aluminium plate display several sharp peaks characteristic of a sample with large grain size. This problem could be overcome by using a larger sample and an oscillator, but for the determination of the fourth coefficients in the orientation distribution function this is not necessary as shown below.

Following Roe (1966), the plane normal orientation distribution function $q(\zeta, \eta)$ may be expanded as a series of spherical harmonics

$$q(\zeta, \eta) = \sum_{l=0}^{\infty} \sum_{m=-l}^{l} Q_{lm} P_l^m(\zeta) \, e^{-im\eta}, \tag{24}$$

where $P_l^m(\zeta)$ is the normalized associated Legendre function. The Q_{lm} are given as integrals over the measured plane normal distribution,

$$Q_{lm} = \frac{1}{2\pi} \int_0^{2\pi} \int_{-1}^{1} q(\zeta, \eta) \, P_l^m(\zeta) \, e^{im\eta} \, d\zeta \, d\eta, \tag{25}$$

and may be written in terms of the coefficients W_{lmn} in (4) as follows

$$Q_{lm} = 2\pi \sqrt{\frac{2}{2l+1}} \sum_{n=-l}^{l} W_{lmn} P_l^m(\Xi) \, e^{in\Phi}, \tag{26}$$

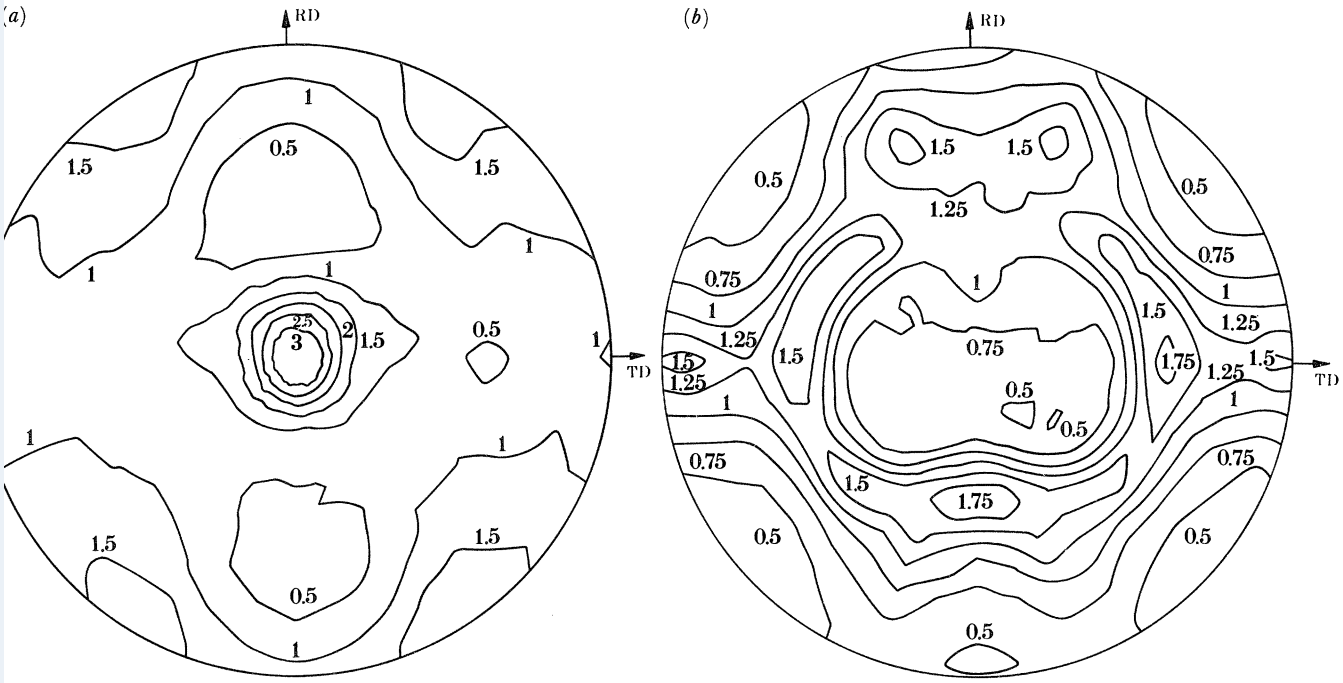

FIGURE 6. Pole figure diagrams for the Al–4.5% Mg plate showing contours of Bragg intensity for (*a*) the (200) reflection and (*b*) the (111) reflection.

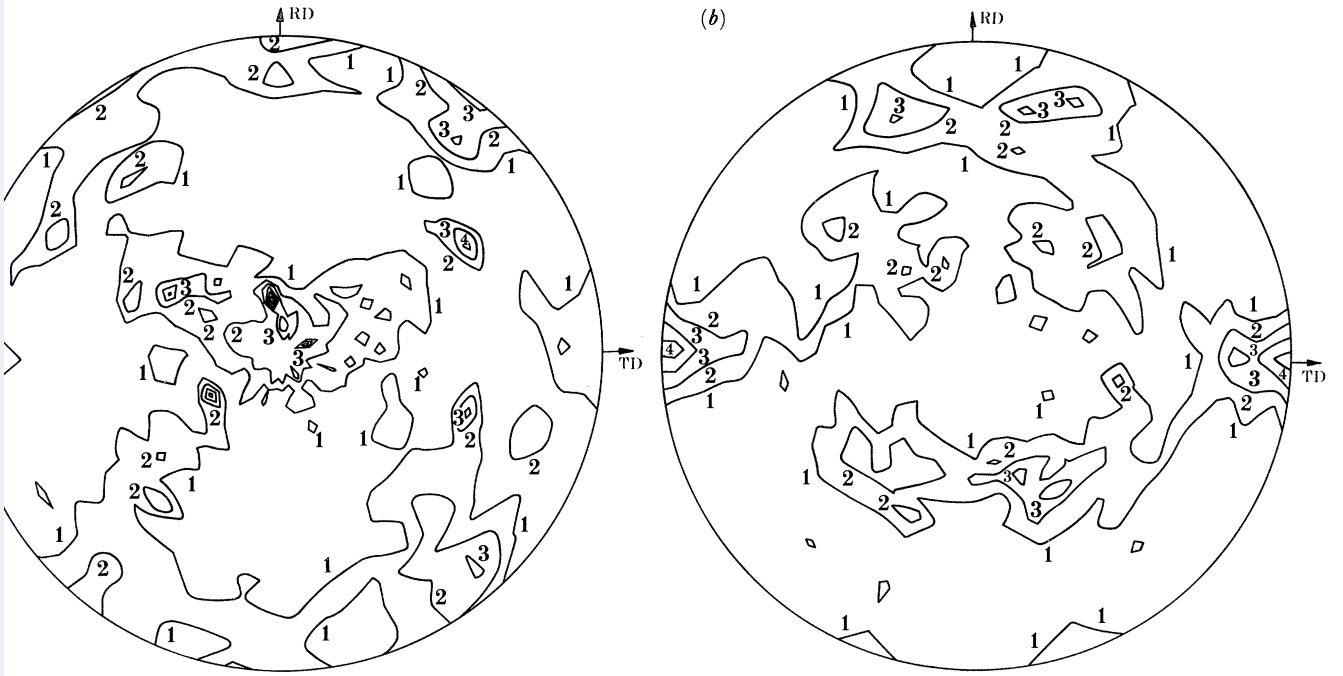

FIGURE 7. Pole figure diagrams for the 99.5% pure aluminium plate showing contours of Bragg intensity for (*a*) the (200) reflection and (*b*) the (111) reflection.

where $\Xi = \cos\Theta$, Θ and Φ being the polar and azimuthal angles of the plane normal, τ, with respect to the crystallite axes $0X_1$, $0X_2$, $0X_3$. Equation (26) is a linear equation with $2l+1$ unknowns for given values of l and m. If measurements are made for $2l+1$ plane normals, and the corresponding Q_{lm} are determined, the $2l+1$ simultaneous linear equations can be solved for the W_{lmn}. This allows the crystallite orientation distribution function to be determined from the measured pole figures.

Each pole figure shown in figures 6 and 7 was used to determine the coefficients Q_{4m} in the expression for the plane normal distribution function. These coefficients are tabulated in the left hand column of table 1. From these, the coefficients W_{4m0} in (4), appropriate for the

TABLE 1. VALUES OF Q_{lm} AND W_{lmn} DETERMINED BY NEUTRON DIFFRACTION

pole figure	Al–4.5% Mg		99.5% pure Al	
(200)	$Q_{40} = 0.04643$	$W_{400} = 0.00739$	$Q_{40} = 0.03563$	$W_{400} = 0.00567$
	$Q_{42} = -0.00974$	$W_{420} = -0.00155$	$Q_{42} = -0.01629$	$W_{420} = -0.00259$
	$Q_{44} = -0.01521$	$W_{440} = -0.00242$	$Q_{44} = -0.01709$	$W_{440} = -0.00272$
(111)	$Q_{40} = -0.03057$	$W_{400} = 0.00730$	$Q_{40} = -0.02540$	$W_{400} = 0.00606$
	$Q_{42} = 0.00691$	$W_{420} = -0.00165$	$Q_{42} = 0.01037$	$W_{420} = -0.00247$
	$Q_{44} = 0.01014$	$W_{440} = -0.00242$	$Q_{44} = 0.01117$	$W_{440} = -0.00267$

calculation of the ultrasonic velocities, were calculated and are given in the right-hand column of table 1. The results of each sample from two different pole figures are in good agreement despite the large grain size of the 99.5% pure aluminium plate. This is a result of the low angular sensitivity of the fourth order Legendre functions appearing in (25) for the calculation of the Q_{4m}. An average over the (200) and (111) pole figures gives $\overline{W}_{400} = 0.00587$, $\overline{W}_{420} = -0.00253$ and $\overline{W}_{440} = -0.00269$ for the aluminium 4.5% magnesium plate and $\overline{W}_{400} = 0.00734$, $W_{420} = -0.00160$ and $W_{440} = -0.00242$ for the 99.5% pure aluminium plate. The values for W_{420} and W_{440} are in reasonable agreement with the values determined by ultrasonics listed in the previous section.

5. CONCLUSION

In this paper it has been shown that for a plate with homogeneous texture, surface-Rayleigh-wave velocity measurements can be combined with the normal shear-wave birefringence technique to give a texture independent determination of the difference in principal stresses in the plane of the plate. This is given by (20). The theory is based on an analytical expression, (7), for the angular dependence of the Rayleigh-wave velocity in polycrystalline metals with small anisotropy typical of rolled plate. This was derived by writing the crystallite orientation distribution function of the sample as a linear combination of generalized Legendre functions, (4), with expansion coefficients W_{lmn}. Only the coefficients W_{400}, W_{420} and W_{440} are required to calculate the ultrasonic velocity. The theory was tested by obtaining these coefficients in two independent ways. First W_{420} and W_{440} were determined from the velocity of bulk waves and the predicted variation of the Rayleigh-wave velocity using these values was compared with the observed frequency dependence. Secondly, neutron diffraction was used to obtain these coefficients for lcm³ samples cut from the plates. The measured values are summarized in table 2 and are in reasonable agreement with those obtained from the bulk

PHILOSOPHICAL TRANSACTIONS OF THE ROYAL SOCIETY A MATHEMATICAL, PHYSICAL & ENGINEERING SCIENCES

TABLE 2. COMPARISON OF VALUES OF W_{400}, W_{420} AND W_{440} DETERMINED BY ULTRASONICS WITH THOSE DETERMINED BY NEUTRON DIFFRACTION

99.5% pure Al	W_{400}	W_{420}	W_{440}
ultrasonics	—	−0.002267	−0.002560
(200)	0.005671	−0.0025925	−0.0027206
(111)	0.0060636	−0.0024745	−0.0026664
Al–4.5% Mg	W_{400}	W_{420}	W_{440}
ultrasonics	—	−0.001721	−0.003060
(200)	0.0073897	−0.0015506	−0.002420
(111)	0.0072983	−0.0016496	−0.0024196

measurements showing that the theory for the ultrasonic velocities in terms of W_{400}, W_{420} and W_{440} is accurate. However, the Rayleigh-wave velocity was found to be frequency dependent. This is due either to a surface texture or stress different from the bulk value, the velocity only agreeing with the prediction based on bulk velocity measurements in the limit of low frequency. As a result the combination of the Rayleigh-wave velocity with either a skimming-sv or longitudinal wave would be more satisfactory. The velocities of these waves need to be measured at a frequency at which the waves average over depth in the same way as the Rayleigh wave. This should allow the depth profile of the texture and stress to be determined from the frequency dependence of the Rayleigh-wave velocity.

REFERENCES

Aki, K. & Richards, P. G. 1980 *Quantitative seismology. Theory and methods*, volume I, pp. 286–298. San Francisco: W. H. Freeman and Company.

Allen, A. J., Hutchings, M. T., Sayers, C. M., Allen, D. R. & Smith, R. L. 1983 *J. appl. Phys.* **54**, 555–560.

Allen, D. R. & Cooper, W. H. B. 1983 AERE report R-10933.

Bunge, H. J. 1965 *Z. Metallk.* **56**, 872–874.

Bunge, H. J. 1968 *Krist. Tech.* **3**, 431–438.

Davies, G. J., Goodwill, D. J. & Kallend, J. S. 1972 *Metall. Trans.* **3**, 1627–1631.

Hatherley, M. & Hutchinson, W. B. 1979 *An introduction to textures in metals*, monograph no. 5. London: Institution of Metallurgists.

Hayes, M. & Rivlin, R. S. 1961 *Arch. ration Mech. Analysis* **8**, 358–380.

Hirao, M., Fukuoka, H. & Hori, K. 1981 *J. appl. Mech.* **48**, 119–123.

Hsu, N. N. 1974 *Expl Mech.* **14**, 169–176.

Hutchinson, W. B. 1984 *Int. metall Rev.* **29**, 25–42.

Jeffreys, H. 1961 Geophys. *Jl R. astr. Soc.* **6**, 115–117.

Langman, R. & Allen, D. R. 1985 AERE Report R-11598.

Morris, P. R. 1969 *J. appl. Phys.* **40**, 447–448.

Pursey, H. & Cox, H. L. 1954 *Phil. Mag.* **45**, 295–302.

Roe, R. J. 1965 *J. appl. Phys.* **36**, 2024–2031.

Roe, R. J. 1966 *J. appl. Phys.* **37**, 2069–2072.

Roe, R. J. & Krigbaum, W. R. 1964 *J. chem. Phys.* **40**, 2608–2615.

Sayers, C. M. 1982 *J. Phys.* D **15**, 2157–2167.

Sayers, C. M. 1985 *Proc. R. Soc. Lond.* A **400**, 175–182.

Smith, M. L. & Dahlen, F. A. 1973 *J. geophys. Res.* **78**, 3321–3333.

Stickels, C. A. & Mould, P. R. 1970 *Met. Trans.* **1**, 1303–1312.

Discussion

H. N. G. WADLEY (*A*163, *Materials Building*, 223, *NBS, Gaithersburg, Maryland, U.S.A.*). Texture is a depth-dependent property in plate materials and thus makes a contribution to the Rayleigh velocity that varies with frequency. Methods have been developed (for example,

see Aki & Richards (1980) to invert Rayleigh-wave dispersion data to deduce the depth dependence of an effective elastic modulus. Has Dr Sayers given consideration to this approach?

C. M. Sayers. The dominant contribution to the frequency dependence of the Rayleigh-wave velocity shown in figure 5 arises from the variation in texture with depth. I have only recently begun to address the inverse problem of obtaining the depth profile from the frequency dependence, and have assumed the type of profile (e.g. Gaussian, exponential or step) is known. A more satisfactory inversion procedure could presumably be developed by using the maximum entropy method, and I plan to examine this.

R. B. Thompson (*Ames Laboratory, Iowa State University, Ames, Iowa, U.S.A.*). Let me first comment that the problem of inverting Rayleigh-wave dispersion data to predict gradients on physical properties has been considered by J. M. Richardson and colleagues at the Rockwell International Science Center. They considered the cases in which the data was sparse (measurements at a few frequencies) and dense (measurements at many frequencies). Brief accounts of the work have been included in the Proceedings of the Ultrasonics Symposium (IEEE, U.S.) in the mid-1970s. I do not recall the exact citations where the more complete discussions have been presented.

My question regards Dr Sayers' texture-independent expression for the difference in the principal strains. It would appear that the acoustoelastic constant α_1/α_0 should depend on texture. How is this handled in his application of the formula?

Also, in the theory which Dr Sayers has presented it is assumed that the material is a single-phase polycrystal. Has he made any experimental observations on materials containing second phases? If so, to what extent did this simple theory provide useful guidelines?

C. M. Sayers. Thank you for the references (Richardson *et al.* 1977, 1978). These papers treat the case of an isotropic medium, but I see no difficulty in generalizing the approach to propagation along the principal texture axes of the elastic constant tensor. The situation is much more complicated for off-axis propagation in a strongly textured material when the plane of polarization rotates out of the sagittal plane. In reply to the question, I have assumed the effect of texture on the acoustoelastic response to be of higher order than the terms considered here. This is true for shear waves in a plate of mild steel, where the difference in the acoustoelastic effect for a stress applied parallel and perpendicular to the rolling direction was found to be small (Sayers & Allen 1984, figure 4). For strongly textured materials such as austenitic welds, however, I would expect cross terms to be important.

The sample of steel considered by Sayers & Allen (1984) consists of ferrite and pearlite as shown in figure 3*b* of Allen & Sayers (1984). The [110] pole figure for this sample is shown in figure 1 of Allen & Sayers (1984) and gives the value $W_{420} = -0.00014$. This predicts a shear-wave birefringence $(v_{31} - v_{32})/v_S^0 = 0.22\,\%$, which compares with the measured value of 0.19% (Sayers & Allen, 1984). This discrepancy falls within the error of the pole figure determination which is much less accurate than the ultrasonic velocity measurement. For austenitic cladding containing 12% δ-ferrite the values of W_{400}, W_{420} and W_{440} obtained from pole figure measurements (Allen *et al.* 1983) correctly describe the angular dependence of the ultrasonic velocities. We have made no measurements on samples containing volume fractions of a second phase greater than these.

PHILOSOPHICAL TRANSACTIONS OF THE ROYAL SOCIETY A MATHEMATICAL, PHYSICAL & ENGINEERING SCIENCES

References

Allen, D. R. & Sayers, C. M. 1984 *Ultrasonics* **22**, 179–188.
Allen, D. R. 1983 *J. appl. Phys.* **54**, 555–560.
Richardson, J. M. 1977 *J. appl. Phys.* **48**, 498–512 and 5111–5121.
Richardson, J. M. 1978 *J. appl. Phys.* **49**, 5242–5249.
Sayers, C. M. & Allen, D. R. 1984 *J. Phys.* D **17**, 1399–1413.

E. Almond (*National Physical Laboratory, Teddington, Middlesex, U.K.*). This point is with relation to the effect of second phases in metal steels; the microstructure often consists of alternate layers of cold-worked textured material separated by recrystallized layers. There may also be layers of pearlite, which has completely different properties than the steel, present. How will these constituents affect Dr Sayers' measurements? They are important because they represent the 'real' structure of many steels.

C. M. Sayers. The microstructure of the steel considered by Sayers & Allen (1984) is shown in figure 3*b* of Allen & Sayers (1984). The structure consists of ferrite (light areas) and pearlite (dark areas). To within the accuracy of the pole figure determination, however, the measured anisotropy of the ultrasonic velocities is consistent with the prediction of the theory. I should emphasize that the bcc Fe [110] pole figure presented for this sample in figure 1 of Allen & Sayers (1984) represents the texture of bcc iron averaged over the ferritic and pearlitic regions. A further effect of the microstructure is grain scattering which gives a frequency dependent velocity and attenuation of the ultrasonic wave. However, the frequency dependence of the ultrasonic velocity due either to grain boundary scattering or to scattering by second phases is small compared to the velocity dispersion shown in figure 5 (Allen *et al.* 1982). Nevertheless, the angular variation of this contribution has been suggested as an alternative for separating out the effects of texture and stress in the shear wave birefringence technique by Goebbels & Hirsekorn (1984).

References

Allen, D. R., Cooper, W. H. B., Sayers, C. M. & Silk, M. G. 1982 In *Research techniques in nondestructive testing* (ed. R. S. Sharpe), pp. 151–209, vol. 6. New York: Academic Press.
Goebbels, K. & Hirsekorn, S. 1984 *Non.-destruct. Test. Int.* **17**, 337–342.

PHILOSOPHICAL TRANSACTIONS OF THE ROYAL SOCIETY A MATHEMATICAL, PHYSICAL & ENGINEERING SCIENCES